

Total Yield Measurements in $^{23}\text{Na}(\text{p}, \gamma)^{24}\text{Mg}$

Z. E. Switkowski,^{A,B} R. O'Brien,^{A,C} A. K. Smith^A and D. G. Sargood^A

^A School of Physics, University of Melbourne, Parkville, Vic. 3052.

^B Present address: California Institute of Technology, Pasadena, California, U.S.A.

^C Present address: State College of Victoria at Melbourne, Parkville, Vic. 3052.

Abstract

The reaction $^{23}\text{Na}(\text{p}, \gamma)^{24}\text{Mg}$ has been investigated in the proton energy range 0.25–2.5 MeV. Total γ -ray strengths were determined for 64 resonances. A yield curve was measured over the range 0.65–2.55 MeV, and an estimate of the nonresonant cross section was obtained. Total resonance widths were deduced for 32 levels.

1. Introduction

The role played by the photodisintegration of ^{24}Mg in influencing the rate of synthesis of heavier elements during the latter stages of stellar evolution has been considered by several authors in the contexts of quiescent silicon burning (Bodansky *et al.* 1968; Michaud and Fowler 1972) and explosive processes (Arnett and Truran 1969; Arnett 1969; Woosley *et al.* 1973). For temperatures in the range $1 < T_9 < 5$ (where T_9 is the temperature measured in units of 10^9 K), which is appropriate to silicon burning, the photodisintegration of ^{24}Mg proceeds primarily through the (γ, α) and (γ, p) reactions. Fowler and Hoyle (1964) showed how such reaction rates may be determined from a study of the inverse processes and the application of the reciprocity theorem. In this way photodisintegration of ^{24}Mg nuclei in excited states may be correctly estimated, providing the states are in thermodynamic equilibrium.

The $^{20}\text{Ne}(\text{p}, \gamma)^{24}\text{Mg}$ reaction has been investigated over the astrophysically relevant energy range by Smulders (1965) and, more recently, by Couch and Shane (1971). Using the data published in the review article by Endt and Van der Leun (1967), which contained information on resonances in $^{23}\text{Na}(\text{p}, \gamma)^{24}\text{Mg}$ up to only 1.46 MeV proton energy, Couch and Shane then calculated that at $T_9 = 5$, a temperature readily reached during Si burning, the photodisintegration rate via the (γ, p) channel rises to as much as 26% of the total photodisintegration rate of ^{24}Mg . As the range of effective stellar energies (see Fowler and Hoyle 1964; Clayton 1968) for the $^{23}\text{Na}(\text{p}, \gamma)^{24}\text{Mg}$ reaction corresponding to the temperature range $1 < T_9 < 5$ is from 0.3 to 2.7 MeV, experimental determination of all resonance strengths in this energy region, together with an estimate of any nonresonant yield, is required for accurate calculations of photodisintegration rates.

At the outset of the present work, the most comprehensive investigations of the $^{23}\text{Na}(\text{p}, \gamma)^{24}\text{Mg}$ reaction were: Nordhagen and Steen (1964) who measured the strengths of 20 resonances in the proton range 0.87–1.46 MeV, Prosser *et al.* (1962) who made measurements on 12 resonances in the range 0.58–1.42 MeV, and Glaudemans and Endt (1962, 1963) who obtained absolute strengths for 8

resonances below 750 keV. There was disagreement between the results of Glaudemans and Endt and those of Prosser *et al.* in the energy region of overlap. Several other groups have also studied this reaction (Wagner and Heitzmann 1960; Berkes *et al.* 1964; L'Ecuyer and Levesque 1966; Baxter *et al.* 1969). More recently, Meyer *et al.* (1972) published the strengths of 16 resonances in the range 0.98–1.86 MeV. No strengths were measured for resonances above 1.86 MeV.

It was therefore determined to measure resonance strengths over as much of the range of energies of stellar interest as possible, namely from 0.25 to 2.7 MeV. However, excessive count rates from $^{23}\text{Na}(\text{p}, \text{p}'\gamma)$ limited the range of energies actually investigated to that from 0.25 to 2.5 MeV.

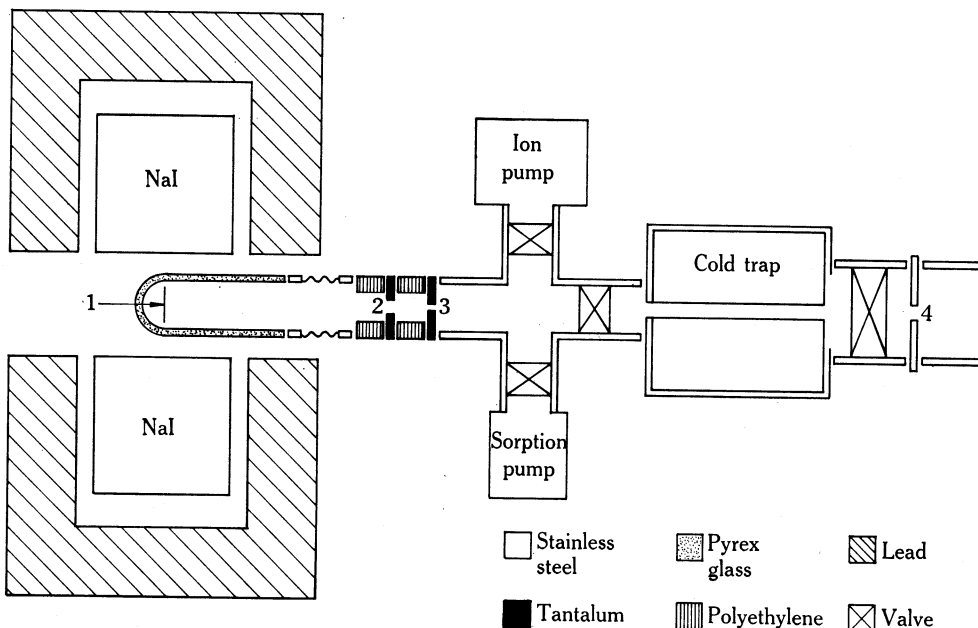


Fig. 1. Schematic diagram of the experimental apparatus, showing: 1, target; 2, electron suppressor; 3 and 4, beam defining apertures. The NaI crystals were shielded with 10 cm of lead.

2. Experimental Details

The present experiment was performed with proton beams from the University of Melbourne 800 kV electrostatic accelerator and the 3MV Van de Graaff accelerator of the Australian Atomic Energy Commission. The 800 kV accelerator has a 90° analysing magnet, and beam energy resolution was maintained at ± 2 keV by entrance and exit slits. The 3 MV accelerator has a 25° analysing magnet, and beam defining slits and collimators held the energy spread to less than ± 0.5 keV. A schematic diagram of the beam line is shown in Fig. 1. A 50 cm long by 0.8 cm internal diameter stainless steel liquid nitrogen trap isolated the beam tube from the target system. Before striking the target the beam was defined by a grounded 0.3 cm diameter tantalum aperture, which was followed by an electron suppressor ring maintained at -600 V.

It was not possible to work with elemental sodium targets, owing to deterioration under bombardment and surface oxidation. However, targets suitable for measure-

ment of relative strengths by means of thin target excitation functions were made by evaporating 99.93% spectroscopically pure sodium (supplied by E. Merck Ltd, Darmstadt, Germany) onto 0.025 cm thick tantalum discs and then transferring these targets at a pressure of 10^{-5} torr to the target chamber where they were deliberately oxidized in an atmosphere of dry oxygen. Yield measurements on chosen resonances showed that the composition of these targets remained unchanged during extended runs. Semi-thick targets were prepared by evaporating 99.99% pure NaBr *in vacuo* onto gold or tantalum blanks. These NaBr targets were transferred under a dry argon or nitrogen atmosphere. No resulting ^{15}N contamination was ever observed. A test of target purity is described in Section 4a below. The targets were held by air pressure on the end of the target chamber, with the 'O' ring seal between the target and the chamber forming an integral part of the vacuum system, which was pumped by a 20 l s^{-1} ion pump to a pressure of 7×10^{-7} torr. The presence of an ungreased Viton 'O' ring near the target did not introduce any significant carbon contamination.

3. Detection System

Since the aim of the present experiment was to measure total γ -ray yields, the two-crystal sum spectrometer technique of Lyons *et al.* (1969) was used. Two 12.70×15.24 cm NaI detectors were arranged face to face 24 mm apart, with the target centred between them. The gains in the two detection channels were matched and the amplified outputs were summed and then analysed by either a Technical Measurement Corporation 256-channel multichannel analyser or a Digital Equipment Corporation PDP-7 on-line computer.

The summed signal was also fed into two single channel analysers (SCA_1 and SCA_2) each of which drove a scaler. The output of SCA_1 was also used to gate the ADC. The window of SCA_1 covered the range 1–15 MeV, thereby enabling the highest energy γ -ray of interest to be analysed while excluding the low energy background and pulses from the $^{23}\text{Na}(\text{p}, \text{p}'\gamma)^{23}\text{Na}$ reaction which was of no interest but whose analysis could contribute significantly to the dead time of the analyser. The total count from SCA_1 was used to determine the fractional live time of the ADC. At the count rates tolerated in this experiment, dead time losses within SCAs or scalers were completely negligible by comparison with the ADC dead time, so that the fractional live time was equal to the ratio of the integrated count recorded by the analyser to the SCA scaler count.

The single channel analyser SCA_2 was used to measure excitation functions. It recorded only those pulses in the energy range 7.8–15.0 MeV, thereby excluding any contributions from the very common contamination reaction $^{19}\text{F}(\text{p}, \alpha\gamma)^{16}\text{O}$. The beam current was integrated by an Elcor A308C integrator which controlled the whole detection circuitry.

4. Yield Measurement

(a) *Semi-thick Target Yield Measurements*

When resonance widths and spacing permitted, strengths were obtained by measuring the step height in the yield from semi-thick NaBr targets. Excitation functions were traced out over resonances in 1 or 2 keV steps, with spectra being accumulated at each point, typically for $100\text{ }\mu\text{C}$ of integrated charge. Beam currents between 0.2 and $2.0\text{ }\mu\text{A}$ were used, depending on the yield, and the dead time in the ADC

was kept below 10%. The yield at each point was corrected for the time-dependent target-independent room background. This background was measured with the beam striking a beam stop located 4 m upstream from the target. The spectrum shape for each resonance was obtained by recording spectra at two different energies (separated by 1–3 keV) on the rising edge of the semi-thick target step and, after correcting each for room background, taking their difference. This procedure produced a spectrum that was free from all but the most rapidly varying background. The total number N_i of interactions with the NaI detectors, corresponding to the step in the yield function, was then given by the integrated spectrum count normalized by the scaler readings. However, since the measured spectra contained no points below 1 MeV, before the integrated spectrum could be obtained, a method was needed for effectively extrapolating the spectrum to zero energy. The lowest energy γ -ray in the spectra was at 1.37 MeV, and the adopted method consisted of extrapolating to zero energy the general trend above the 1.37 MeV photopeak and calculating the 1.37 MeV contribution to the integrated spectrum from its photopeak area, measured above this extrapolation, and its photofraction.

The photofraction was determined from a study of the 512 keV resonance. The decay scheme of this resonance has been accurately determined by a number of workers (Glaudemans and Endt 1962, 1963; Meyer *et al.* 1972; Boydell 1973) and is well known. The 1.37 MeV state is fed by 85% of decays. Given this information, it is possible to determine the strength of the 512 keV resonance by analysing either the whole γ -ray spectrum or just the 1.37 MeV spectrum. The demand that both analyses yield the same resonance strength fixes the 1.37 MeV photofraction within quite narrow limits. This measurement was carried out using a single NaI crystal at 10 cm and an angle of 55°. Calculation of the increased probability of detecting Compton scattered photons in the two-crystal close geometry indicated that the photofraction would be increased by 4%. The finally adopted value was 0.57 ± 0.07 . Analysis of the two-crystal spectrum, using this value of the photofraction, yielded a resonance strength in good agreement with the single crystal value. This value of the photofraction is consistent with that obtained by Ahmed *et al.* (1971) for the same size detector and with that obtained by Marion and Young (1968) whose data were for 12.70×12.70 cm detectors but which would not be expected to have significantly different photofractions.

At some resonances there was a significant contribution from the $^{23}\text{Na}(\text{p}, \alpha_1 \gamma)^{20}\text{Ne}$ reaction producing a pronounced 1.63 MeV γ -ray peak in the spectrum. This contribution was excluded from the analysis by fitting the low energy portion of the spectrum with a sum of 1.37 and 1.63 MeV line shapes and then subtracting the $(\text{p}, \alpha_1 \gamma)$ component. The uncertainties in the extrapolation procedure, photofractions, and 1.63 MeV interference resulted in a typical error of $\pm 4\%$ in N_i .

The step in a thick target excitation function is given by

$$\gamma(\infty, \infty) = N_i/\epsilon_t, \quad (1)$$

where ϵ_t , the probability of any interaction with the NaI detectors, is given by

$$\epsilon_t = \sum_i \beta_i \left(1 - \prod_{j=1}^n \{1 - \epsilon(E_{ji})\} \right), \quad (2)$$

β_i is the branching ratio for each cascade ($\sum_i \beta_i = 1$), n_i is the number of members in

the i th cascade, E_{ji} is the energy of the j th member of the i th cascade, and $\epsilon(E_{ji})$ is the detection efficiency for monoenergetic γ -rays of energy E_{ji} (see Lyons *et al.* 1969). The monoenergetic γ -ray efficiencies were calculated using the attenuation coefficients of Grodstein (1957). The efficiencies were corrected to allow both for attenuation of the γ -rays by the target backing, target chamber and detector housing, and for enhancement of the efficiency due to interactions in the absorbers resulting in the subsequent detection of the secondary products. The uncertainty in $\epsilon(E_{ji})$ was considered to be $\pm 5\%$. Branching ratios were obtained from Endt and Van der Leun (1967), Meyer *et al.* (1972) and Boydell (1973). The uncertainty in the total detection efficiency ϵ_t due to errors in β_i , $\epsilon(E_{ji})$ and angular distribution effects was estimated to be $\pm 5\%$.

The resonance strength is defined (see Gove 1959) as

$$(2J_r + 1) \Gamma_p \Gamma_\gamma / \Gamma = \{A/(A+1)\}^2 (2J_p + 1)(2J_t + 1) \pi^{-2} \hbar^{-2} M_p E_r \xi(E_r) y(\infty, \infty), \quad (3)$$

where J_p , J_t and J_r are respectively the spins of the proton, the target nucleus and the resonant level through which the reaction proceeds; Γ_p , Γ_γ and Γ are respectively the proton, γ -ray and total widths of the resonance level; A is the mass number of the target nucleus; M_p is the proton mass; E_r is the resonance energy; and $\xi(E_r)$ is the target atomic stopping power measured at the resonant energy E_r .

The absolute strengths were calculated using values of ξ from the compilation of Marion and Young (1968) and assuming a knowledge of the stoichiometric composition of sodium bromide targets. To establish confidence in the resonance strengths determined in this manner, one of the absolute resonance strengths was also measured with a pure elemental target to provide a calibration standard. For this purpose, a piece of sodium was washed in a high-purity low-boiling point petrol and in ethanol, and was then cut into a disc of 1 mm thickness in an atmosphere of dry nitrogen and transferred quickly to the target chamber. The sodium disc constituted a target of effectively infinite thickness. The γ -ray yield was measured over the 309 keV resonance. Contributions from lower energy resonances at 251 and 286 keV would have been constant and less than 0.5% of the 309 keV plateau height. The excitation function indicated the presence of considerable surface oxidation (~ 70 keV at these energies) but a constant plateau persisted for ~ 100 keV above this until the 512 keV resonance was reached. The 339, 374 and 445 keV resonances were too weak to affect this plateau. The resonance strength calculated from this measurement with an elemental target was 0.97 ± 0.10 eV. Strengths measured from two separate semi-thick NaBr targets were 0.98 ± 0.08 and 0.94 ± 0.07 eV, where the quoted errors do not include common uncertainties in the stopping power of sodium and in ϵ_t . It was concluded that accurate resonance strengths could be obtained with the NaBr targets.

The resulting resonance strengths together with those deduced from thin target data (described in subsection (b) below) are shown in Table 1, which summarizes the results obtained for all resonances studied. The errors in the strengths are of the order of 20% or 25% for measurements made with a semi-thick or thin target respectively. No attempt was made to measure resonance energies, and the values adopted in the table are from Stelson and Preston (1954) and Endt and Van der Leun (1973), except for the 2492 keV resonance which has not been reported previously.

As a check on the γ -ray detection efficiency, measurements were made on four resonances in $^{27}\text{Al}(\text{p}, \gamma)^{28}\text{Si}$, using the identical experimental arrangement to that

Table 1. Summary of $^{23}\text{Na}(\text{p},\gamma)^{24}\text{Mg}$ yield data

Resonance energy ^A E_r (keV)	Resonance strength $(2J_r + 1) \Gamma_p \Gamma_\gamma / \Gamma$ (eV)	Method of analysis		Width ^B Γ (keV)
		Thick target	Thin target	
251	0.0048 ± 0.0016	Yes	No	
286	< 0.005	Yes	No	
309	0.97 ± 0.17	Yes	No	
339	< 0.01	Yes	No	
374	0.013 ± 0.004	Yes	No	
445	< 0.01	Yes	No	
512	0.85 ± 0.18	Yes	No	
592	2.16 ± 0.36	Yes	No	
677	5.9 ± 1.0	Yes	Yes	
723	< 0.03	No	Yes	< 1
739	1.10 ± 0.18	Yes	Yes	< 1
744	1.65 ± 0.30	Yes	Yes	< 1
795	0.022 ± 0.009	No	Yes	5
813	< 0.1	No	Yes	
845	< 0.05	No	Yes	
872	8.4 ± 1.7	No	Yes	7.5
919	< 0.1	No	No	
987	2.24 ± 0.41	Yes	Yes	< 1
1009	0.53 ± 0.19	No	Yes	≤ 1
1010	0.42 ± 0.17	No	Yes	≤ 1
1021	14.6 ± 3.3	No	Yes	3.8
1086	0.062 ± 0.022	No	Yes	< 1
1091	0.28 ± 0.06	No	Yes	5
1136	0.38 ± 0.16	No	Yes	25
1164	2.07 ± 0.46	No	Yes	1.4
1174	9.9 ± 3.0	No	Yes	1.8
1205	1.59 ± 0.37	No	Yes	< 1
1210	0.12 ± 0.055	No	Yes	< 1
1255	0.44 ± 0.11	No	Yes	~ 1
1283	9.5 ± 2.5	No	Yes	5.5
1318	38.5 ± 7	Yes	Yes	1.5
1327	< 1	No	Yes	
1331	< 1	No	Yes	
1362	0.2 ± 0.1	No	Yes	< 1
1398	18.1 ± 4.1	Yes	Yes	~ 1
1417	30.5 ± 6.6	No	Yes	≤ 1
1457	11.5 ± 2.5	No	Yes	7
1517	0.09 ± 0.04	No	Yes	≤ 1
1532	0.18 ± 0.07	No	Yes	3
1557	0.17 ± 0.07	No	Yes	4
1638	3.8 ± 1.4	No	Yes	45
1645	0.13 ± 0.06	No	Yes	2
1652	0.27 ± 0.12	No	Yes	5
1726	9.7 ± 2.3	No	Yes	~ 1
1735	< 0.5	No	Yes	
1748	1.65 ± 0.54	No	Yes	~ 1
1802	1.6 ± 0.8	No	Yes	
1808	0.12 ± 0.05	No	Yes	
1831	1.59 ± 0.46	No	Yes	< 1
1860	0.40 ± 0.14	No	Yes	< 1
1869	< 0.1	No	Yes	
1931	3.4 ± 1.2	No	Yes	6.5
2025	0.63 ± 0.16	No	Yes	~ 1
2072	1.60 ± 0.66	No	Yes	7
2170	0.57 ± 0.23	No	Yes	2
2200	2.8 ± 1	No	Yes	8
2223	5.65 ± 2.8	No	Yes	40
2243	0.57 ± 0.28	No	Yes	2.5
2284	2.76 ± 0.74	No	Yes	3
2297	2.9 ± 1.4	No	Yes	15
2340	4.0 ± 1.4	No	Yes	3
2354	6.5 ± 1.7	No	Yes	4
2436	19.3 ± 5.1	No	Yes	4.5
2492 ± 3	12.3 ± 4	No	Yes	6

^A Energies are taken from Stelson and Preston (1954) and Endt and Van der Leun (1973) except at 2492 keV.^B Errors in the widths are of the order of 20% for widths > 2 keV and of the order of 50% for widths < 2 keV.

used for the $^{23}\text{Na}(\text{p}, \gamma)$ measurements, and the results were compared with those of Lyons *et al.* (1969). This comparison is shown in Table 2. The agreement is excellent.

(b) Thin Target Yield Measurements

Relative strengths of resonances in the proton energy range 600–2500 keV were deduced from thin target excitation functions measured with oxidized sodium targets that were 8–15 keV thick for 1 MeV protons. Yield curves over resonances were traced out in 1 or 2 keV steps, this interval increasing to ~ 5 keV where no known resonances existed. Counts were typically recorded for $50 \mu\text{C}$ of charge at each point. Long runs were taken at most resonances to obtain spectra which could be manipulated to give a clean spectral shape. The experimental yield curve, measured with two separate targets is shown in Fig. 2.

Table 2. Resonance strengths in $^{27}\text{Al}(\text{p}, \gamma)^{28}\text{Si}$

Resonance energy ^A E_r (keV)	Resonance strength $(2J_r + 1)\Gamma_p \Gamma_\gamma / \Gamma$	Present work	Resonance strength $(2J_r + 1)\Gamma_p \Gamma_\gamma / \Gamma$ (eV) Lyons <i>et al.</i> ^B
505	0.86 ± 0.10		0.89 ± 0.12
507			
633	3.16 ± 0.33		3.11 ± 0.41
655	1.50 ± 0.31		1.44 ± 0.18
992	22.5 ± 2.7		22.8 ± 2.5

^A Values are taken from Endt and Van der Leun (1973).

^B Lyons *et al.* (1969) gave their results in centre-of-mass coordinates; these have been converted to laboratory coordinates here for comparison.

The ratio of the strengths of two resonances is given by

$$\frac{[(2J_r + 1)\Gamma_p \Gamma_\gamma / \Gamma]_1}{[(2J_r + 1)\Gamma_p \Gamma_\gamma / \Gamma]_2} = \frac{E_1 Y_1}{E_2 Y_2}, \quad (4)$$

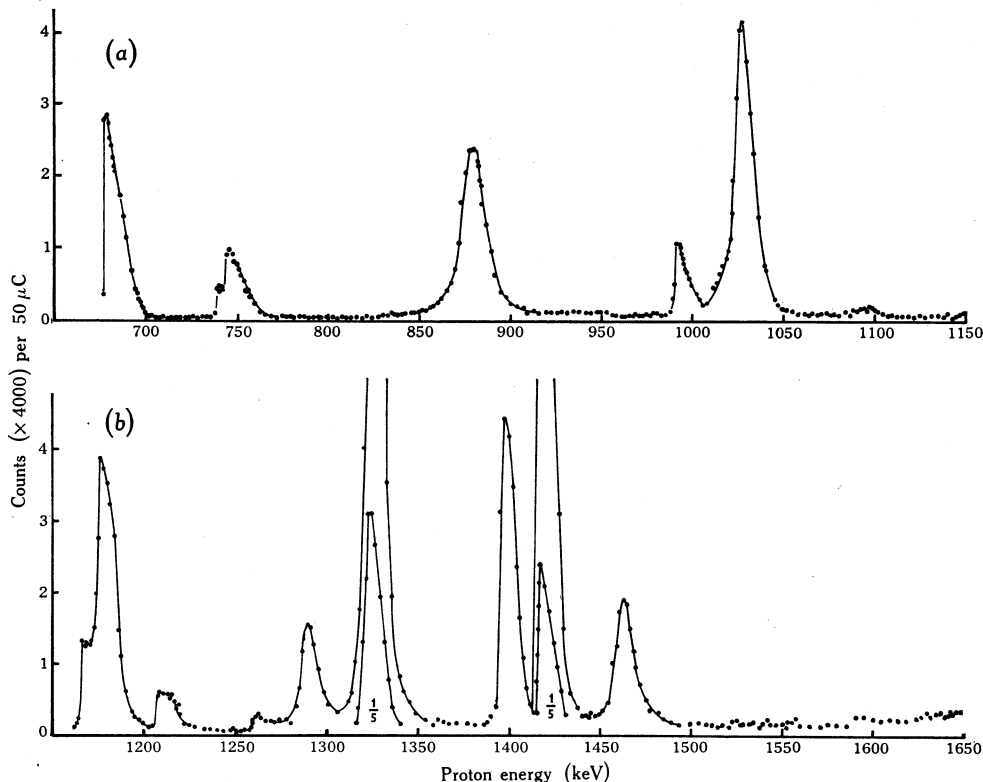
where E_1 and E_2 are the resonance energies, and Y_1 and Y_2 are the integrated yields measured with the same target (see Gove 1959). These yields were determined from the experimental excitation function, as measured by SCA₂, scaled by the fraction of counts that fell in the SCA window, as determined from the pulse height spectrum. At some resonances this fraction could not be directly determined due to the strength of the (p, p'γ) and (p, αγ) reactions or the presence of ^{19}F contamination. Also, useful spectra could not be obtained for very weak or very broad levels. To handle these cases, the concept of partial detection efficiency was used (see Lyons *et al.* 1969).

The partial detection efficiency $\eta(f)$ is defined as the probability that a γ-ray decay of a given resonance results in an interaction with the detectors yielding a pulse height greater than a fraction f of the full energy pulse height E_x . The total number of radiative captures is

$$N = N_i / \varepsilon_t = N'_i(f) / \eta(f), \quad (5)$$

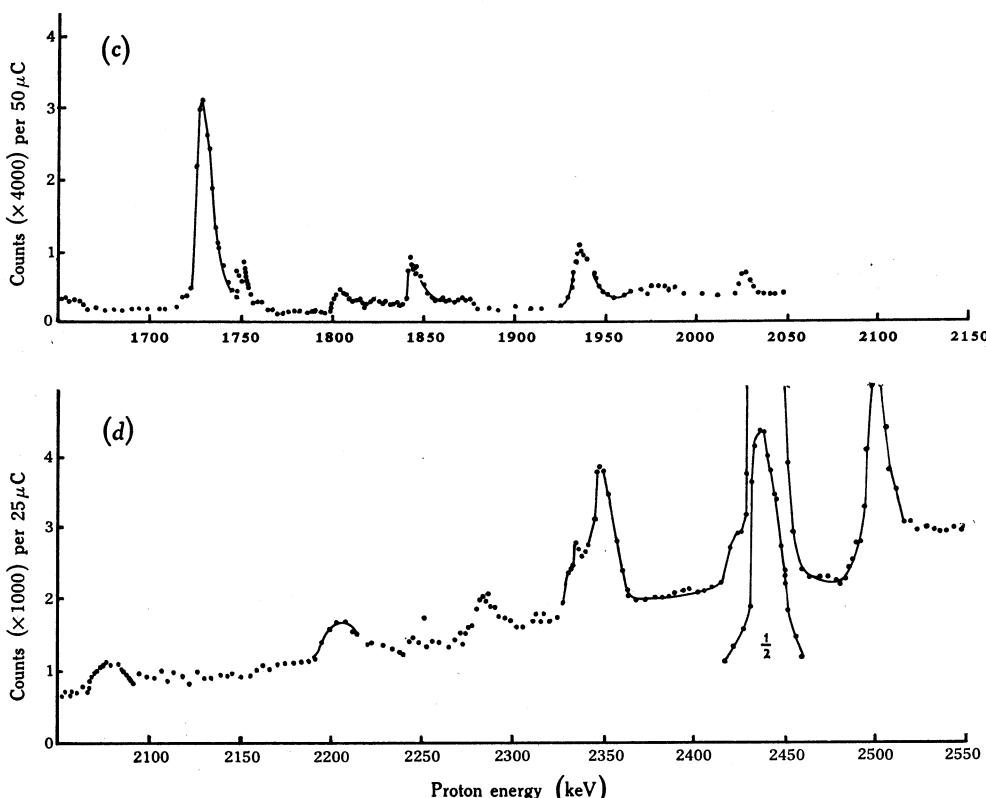
where $N'_i(f)$ is the number of pulses greater than fE_x . The variation of $\eta(f)$ with f was studied for a number of representative resonances including some with simple decay schemes, involving predominantly ground state transitions or two γ-ray cascades, and others with complex decays. A total of 12 spectra measured at

resonances in the $^{23}\text{Na}(\text{p}, \gamma)$ reaction and 3 spectra from the $^{27}\text{Al}(\text{p}, \gamma)$ reaction were studied. As the Q values for the (p, γ) reactions of ^{23}Na and ^{27}Al are nearly equal, the general features of the spectra are similar and the η values are comparable. Typical partial detection efficiency curves are shown in Fig. 3.



Figs 2a and 2b. Experimental yield curve for the reaction $^{23}\text{Na}(\text{p}, \gamma)^{24}\text{Mg}$, with $E_\gamma = 7.8-15.0$ MeV, for proton energies in the range $\sim 700-1650$ keV. The points have been corrected for room background.

The η curves corresponding to different types of cascade structure reach an approximately common point at $f = 0.33$ where $\eta(f) = 0.38 \pm 0.03$. This point corresponds to an energy of ~ 4 MeV so that, when spectra were distorted at low energies due to the $(\text{p}, \alpha\gamma)$ or $(\text{p}, \text{p}'\gamma)$ reactions, this value of $\eta(f)$ could be used in conjunction with the clean spectrum above 4 MeV, regardless of cascade structure. However, this procedure was practical in only a few cases. More often the only usable portions of the spectrum occurred above the peaks from the contaminant $^{19}\text{F}(\text{p}, \alpha\gamma)^{16}\text{O}$ reaction ($E \approx 7.5$ MeV or $f \approx 0.6$) where, as inspection of Fig. 3 shows, the η curves are widely spread. However, from a knowledge of the branching ratios it was possible to determine the value of η usually to an accuracy of $\sim 4\%$. In cases where branching ratios were not known (e.g. for $E_p > 1.86$ MeV) it was generally possible to deduce the value of η from a systematic comparison of the undistorted region of the spectrum with previously analysed clean spectra. When all branching ratio and spectral information was absent, an average value of η was used, and an error of $\pm 20\%$ was then assigned to η .



Figs 2c and 2d. Experimental yield curve for the reaction $^{23}\text{Na}(\text{p}, \gamma)^{24}\text{Mg}$, with $E_\gamma = 7\cdot8-15\cdot0$ MeV, for proton energies in the range 1650-2550 keV. For proton energies greater than 2050 keV, measurements were made with a thicker target. The points have been corrected for room background.

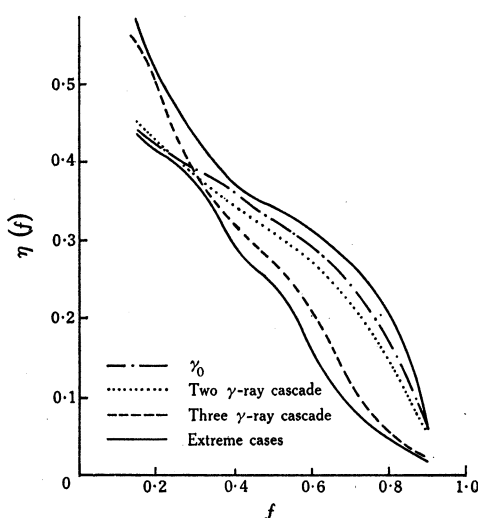


Fig. 3. Typical curves of partial detection efficiency η as a function of the fraction f of excitation energy. Dominant decay modes are indicated in the legend in the diagram. The full curves represent the extreme values of η obtained from all resonances surveyed. The other curves represent averages obtained from many resonances each of which had a common dominant decay mode.

Where contributions from individual resonances were not well resolved, the yield curve was described in terms of an incoherent sum of line shapes each characterized by Breit-Wigner parameters and a common set of experimental resolution factors. More specifically, the γ -ray yield per incident particle at a bombarding energy of E_b for a target of thickness t may be written (Gove 1959)

$$y(E_b, t) = \int_{x=0}^t \int_{E=0}^{E_i} \int_{E_i=0}^{\infty} n(x) \sigma(E) w(E_i, E, x) g(E_b, E_i) dE_i dE dx, \quad (6)$$

where $n(x)$ is the number of target nuclei per unit volume at depth x within the target; $g(E_b, E_i) dE_i$ is the probability that a proton in the incident beam of mean energy E_b will have an energy incident at the target between E_i and $E_i + dE_i$; $w(E_i, E, x) dE$ is the probability that a particle incident on the target with energy E_i will have an energy between E and $E + dE$ at depth x in the target; and $\sigma(E)$ is the nuclear reaction cross section for a proton with energy E .

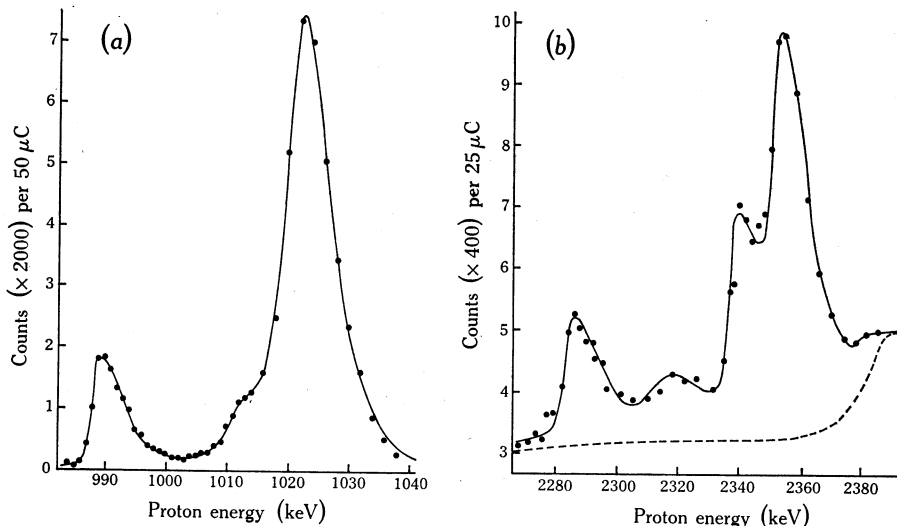


Fig. 4. Typical computed fits of the yield curve to the indicated experimental points. To obtain a satisfactory fit at the higher energies shown in part (b), it was necessary to include a nonresonant component (dashed curve).

The right-hand side of equation (6) was numerically integrated in the following way: $g(E_b, E_i)$ was assumed to be gaussian, $\sigma(E)$ was written as a sum of Breit-Wigner single level expressions, and the straggling function w was obtained from the work of Symon (1952, cited after Rossi 1952) in which the most probable energy loss for charged particles was written as

$$E_b - E_p = 2Cm_0 c^2 x \beta^{-2} |\ln(4Cm_0^2 c^4 x / (1 - \beta^2) I^2(z)) - \beta^2 + j|$$

in the notation of Rossi (1952). For a particular experimental situation, all parameters except x are fixed; and from the family of curves provided by Symon, it is possible to generate the straggling functions $w(E_i, E, x)$. Although these functions are expected to be applicable only at energies greater than 10 MeV (as it is assumed that the velocity of the incoming particle is large compared with the velocities of the

electrons with which collisions occur), previous investigators have successfully fitted (p, γ) yield curves using this approach (see Bondelid and Butler 1963).

Satisfactory fits to the experimental data were obtained with $n(x)$ a linear function which decreased to zero as x increased from 0 to t . Physically this means that the targets were nonuniform, the density of sodium atoms linearly decreasing with depth in the target. Diffusion into, and/or chemical reactions with, the tantalum backing of the oxidized sodium target is qualitatively consistent with these requirements. Typical fits to two separate regions of the yield curve are shown in Fig. 4. The quality of the fits enabled the extraction of many resonance widths greater than ~ 2 keV to an accuracy of $\sim 20\%$. Except in cases where resonances were very close together (<3 keV) or very weak, the error in the fit was the smallest component of the uncertainty in the strength.

Table 3. Comparison of results for $(2J_r + 1)\Gamma_p \Gamma_\gamma / \Gamma$

Resonance energy E_r (keV)	Present results	MRR	Resonance strength (eV)*				GE
			EE	BCK	NS	PUWK	
251	0.0048 ± 0.0016						0.0011 ± 0.0006
309	0.97 ± 0.17						0.36 ± 0.09
374	0.013 ± 0.004						0.009 ± 0.004
512	0.85 ± 0.18						0.30 ± 0.08
592	2.16 ± 0.36						$1.7 \pm 0.69 \pm 0.17$
677	5.9 ± 1.0						$5.6 \pm 2.0 \pm 0.5$
739	1.10 ± 0.18						$1.3 \pm 0.34 \pm 0.09$
744	1.65 ± 0.30						$1.6 \pm 0.45 \pm 0.11$
872	8.4 ± 1.7				9.6 ± 3		5.1
987	2.24 ± 0.41	2		3.2 ± 0.6	4.5 ± 1		2.4
1008	0.53 ± 0.19				1.1 ± 0.7		
1021	14.6 ± 3.3	12		17.2 ± 3.9	14 ± 3	18	
1164	2.07 ± 0.46	3			2.9 ± 0.6	2.2	
1174	9.9 ± 3.0	10		12.9 ± 3.3	13 ± 2.5	11.9	
1205	1.59 ± 0.37	2			1 ± 0.2		
1210	0.12 ± 0.055	0.7					
1255	0.44 ± 0.11	0.9			1.2 ± 0.2		
1283	9.5 ± 2.5	8			7.2 ± 2		
1318	38.3 ± 7.0	46		46 ± 11	53 ± 10	63	
1327	<1	1.5					
1398	18.1 ± 4.1	17			24 ± 5	15.4	
1417	30.5 ± 6.6	34			42 ± 8	40.5	
1457	11.5 ± 2.5	7			12 ± 3		
1726	9.7 ± 2.3	11					
1748	1.65 ± 0.54	2					
1831	1.59 ± 0.46						

* Notes on results:

MRR = Meyer *et al.* (1972); all values are relative to 1.05 eV at the 512 keV resonance; stated errors are $\pm 30\%$.

EE = Engelbertink and Endt (1966).

BCK = Baxter *et al.* (1969); all values are relative to 1.05 eV at the 512 keV resonance.

NS = Nordhagen and Steen (1964).

PUWK = Prosser *et al.* (1962); stated errors are $\pm 15\%$, with which must be compounded any error in the stopping powers compiled by Allison and Warshaw (1953).

GE = Glaudemans and Endt (1962, 1963).

5. Results

(a) Comparison with Other Measurements

Table 3 displays a comparison of the resonance strengths from the present work with those of previous investigators. There is substantial agreement between all authors, with the exception of Glaudemans and Endt (1962, 1963). However, the relative strengths of Glaudemans and Endt are in very good agreement with both the present results and those of Prosser *et al.* (1962). The measurements of Baxter *et al.* (1969)

and Meyer *et al.* (1972) were of relative strengths, which were normalized against the value of 1.05 eV obtained by Engelbertink and Endt (1966) for the 512 keV resonance. The agreement between the present results and the relative strengths of Baxter *et al.* is excellent, while the agreement with the relative strengths of Meyer *et al.* is within the combined errors, except at the 1457 keV resonance, where our value is supported by the work of Nordhagen and Steen, and at the weak 1210 keV resonance. The values of the widths of resonances in the energy range 870–2080 keV are in satisfactory agreement with the results of other authors (Stelson and Preston 1954; Andersen *et al.* 1961; Borgi and Lonsjo 1964; Mourad *et al.* 1967; Meyer *et al.* 1972).

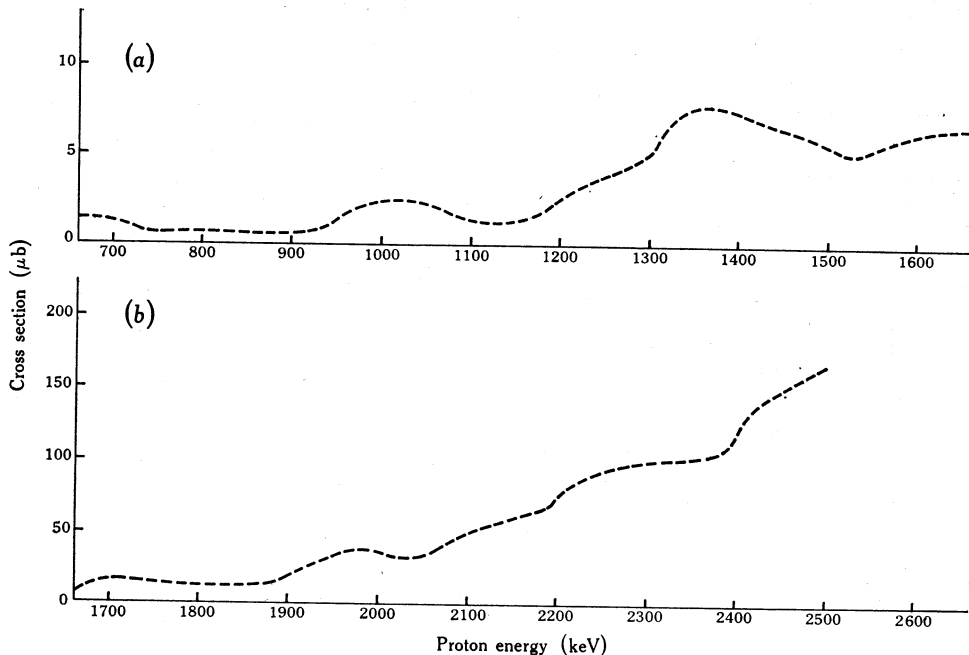


Fig. 5. Unresolved cross section.

(b) Unresolved Yield

Examination of the yield curve plotted in Figs 2a-d indicates the presence of a significant nonresonant yield, particularly at energies greater than 2 MeV. For astrophysical purposes, whether this yield is truly nonresonant or made up of very broad (p, γ) resonances is irrelevant. No attempt was made to identify the structure of this unresolved yield, other than to note that several broad resonances had been observed in this energy region by Stelson and Preston (1954). However, to establish that this yield was due to the $^{23}\text{Na}(p, \gamma)$ reactions and not contaminants (the only likely ones which could produce γ -rays with energies greater than 7.8 MeV being $^{13}\text{C}(p, \gamma)^{14}\text{N}$ and $^{19}\text{F}(p, \gamma)^{20}\text{Ne}$), an excitation function was traced out with a thin NaBr target for proton energies in the range 1.2–2.2 MeV. The fluorine concentration was down by a factor of ~ 20 in this target compared with that in the oxidized sodium targets. The ratio of integrated yields from the two types of target over identical resonances was found to be 1.30 ± 0.13 . The ratio of the off-resonance yields

monitored at five different energies was 1.4 ± 0.2 , where the error fully covers the range of values obtained. This agreement confirms that the unresolved yield arises from reactions with the sodium. This unresolved yield, which was the smoothly varying background that remained after the Breit-Wigner contributions were subtracted, was converted to a cross section and is shown in Fig. 5. The lack of knowledge of the spectral characteristics of this yield necessitated the use of an average value for η in the analysis. An error of $\pm 40\%$ is assigned to this cross section.

Acknowledgments

We would like to thank Dr J. R. Bird for the hospitality of the Australian Atomic Energy Commission Laboratory. This work was supported in part by the Australian Institute for Nuclear Science and Engineering.

References

- Ahmed, N., Awal, M. A., Rahman, M. A., and Khatun, S. (1971). *Nucl. Instrum. Methods* **93**, 381.
 Allison, S. K., and Warshaw, S. D. (1953). *Rev. Mod. Phys.* **25**, 779.
 Andersen, S. L., Dorum, O., Gautvik, E., and Holtebekk, T. (1961). *Nucl. Phys.* **22**, 245.
 Arnett, W. D. (1969). *Astrophys. J.* **157**, 1369.
 Arnett, W. D., and Truran, J. W. (1969). *Astrophys. J.* **157**, 339.
 Baxter, A. M., Cassell, K. J., and Kuehner, J. A. (1969). *Can. J. Phys.* **47**, 2319.
 Berkes, I., Dezhi, I., Kestkheli, L., and Fodor, E. (1964). *Sov. Phys. JETP* **18**, 1186.
 Bodansky, D., Clayton, D. D., and Fowler, W. A. (1968). *Astrophys. J. Suppl. Ser.* **16**(148), 299.
 Bondelid, R. O., and Butler, J. W. (1963). *Phys. Rev.* **130**, 1078.
 Borgi, A. W., and Lonsjo, O. (1964). Internal Rep. Univ. Oslo, Norway.
 Boydell, S. G. (1973). Ph.D. Thesis, University of Melbourne.
 Clayton, D. D. (1968). 'Principles of Stellar Evolution and Nucleosynthesis' (McGraw-Hill: New York).
 Couch, R. G., and Shane, K. C. (1971). *Astrophys. J.* **169**, 413.
 Endt, P. M., and Van der Leun, C. (1967). *Nucl. Phys. A* **105**, 1.
 Endt, P. M., and Van der Leun, C. (1973). *Nucl. Phys. A* **214**, 1.
 Engelbertink, G. A. P., and Endt, P. M. (1966). *Nucl. Phys.* **88**, 12.
 Fowler, W. A., and Hoyle, F. (1964). *Astrophys. J. Suppl. Ser.* **9**(91), 201.
 Glaudemans, P. W. M., and Endt, P. M. (1962). *Nucl. Phys.* **30**, 30.
 Glaudemans, P. W. M., and Endt, P. M. (1963). *Nucl. Phys.* **42**, 367.
 Gove, H. E. (1959). In 'Nuclear Reactions', Vol. 1 (Eds P. M. Endt and M. Demeur), p. 259 (North-Holland: Amsterdam).
 Grodstein, G. W. (1957). X-ray attenuation coefficients from 10 keV to 100 MeV, Nat. Bur. Stand. (U.S.) Circ. 583.
 L'Ecuyer, J., and Levesque, R. J. A. (1966). *Can. J. Phys.* **44**, 2201.
 Lyons, P. B., Toews, J. W., and Sargood, D. G. (1969). *Nucl. Phys. A* **130**, 1.
 Marion, J. B., and Young, F. C. (1968). 'Nuclear Reaction Analysis' (North-Holland: Amsterdam).
 Meyer, M. A., Reinecke, J. P. L., and Reitmann, D. (1972). *Nucl. Phys. A* **185**, 625.
 Michaud, G., and Fowler, W. A. (1972). *Astrophys. J.* **173**, 157.
 Mourad, W. G., Nielsen, K. E., and Petrilak, M. (1967). *Nucl. Phys. A* **102**, 406.
 Nordhagen, R., and Steen, H. B. (1964). *Phys. Norv.* **1**, 239.
 Prosser, F. W., Unruh, W. P., Wildenthal, B. H., and Krone, R. W. (1962). *Phys. Rev.* **125**, 594.
 Rossi, B. (1952). 'High Energy Particles' (Prentice-Hall: Englewood Cliffs, N.J.).
 Smulders, P. J. M. (1965). *Physica (Utrecht)* **31**, 973.
 Stelson, P. H., and Preston, W. M. (1954). *Phys. Rev.* **95**, 973.
 Wagner, S., and Heitzmann, M. (1960). *Z. Naturforsch. A* **15**, 74.
 Woosley, S. E., Arnett, W. D., and Clayton, D. D. (1973). *Astrophys. J. Suppl. Ser.* **26**(231), 231.

